

VibGrasp: Spatiotemporal Vibration Based Multimodal Haptic Rendering with a Lightweight Exo-Glove for 3D Shape Perception

Hojeong Lee, *Graduate Student Member, IEEE*, Eunho Kim, Rachel Kim, Sang Ho Yoon, *Member, IEEE*

Abstract—Haptic feedback has been employed to enhance shape perception during grasp interactions, improving immersion and task performance in extended reality (XR). Although wearable devices offer precise multi-phalangeal haptic feedback, their bulkiness and complexity often hinder practicality. In addition, fingertip-based tactile feedback often limits users’ ability to perceive a continuous and sequential sensation across the finger surfaces during power grasp. We present VibGrasp, a haptic shape-rendering method and a supporting haptic glove that synchronizes spatiotemporal vibrotactile feedback across multiple phalanges with 1-DOF kinesthetic feedback. Using the funneling illusion and duration-modulated vibration patterns, our approach delivers sequential, continuous sensations along the finger to render various shapes. We also develop a lightweight exoskeleton glove with two dorsal-mounted vibration actuators designed to transmit feedback to the ventral surfaces without obstructing motion. Two perception studies demonstrated consistent shape associations and clear preferences for specific patterns. A VR user-experience study further showed that our method achieved higher ratings for realism, satisfaction, and harmony than prior approaches. These findings offer insights into improving immersive and efficient haptic shape rendering in XR.

Index Terms—3D shape perception, funneling, phantom sensation, haptic glove, virtual reality

I. INTRODUCTION

AS extended reality (XR) technology advances, users increasingly demand realistic and immersive experiences within the XR environment. Such facets are commonly achieved by manual interactions with virtual objects. One common example is grasping objects. During the interaction, haptic feedback plays a key role in how humans perceive the object properties, leading to enhanced immersion and improved performance. Therefore, a number of devices have been employed for realistic grasp by providing haptic feedback, including force feedback [1], [2], [3] or tactile stimulation [4], [5], [6] on fingertips, and by adjusting overall hand posture through hand-held [7], [8] or wearable devices [9], [10].

To focus on the role of grasping in shape perception, users commonly perceive object shape through two grasp types [11]: precision grasps, which require fine fingertip manipulation, and power grasps, which involve all phalanges to achieve a robust grip [11], [12], [13]. The realistic reproduction of power

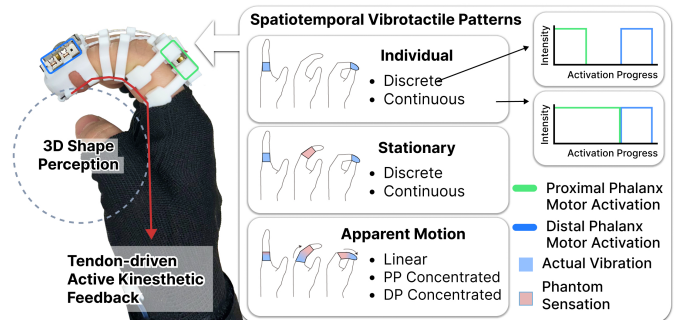


Fig. 1. Proposed haptic rendering method utilizing spatiotemporal vibrotactile patterns with tendon-based 1-DOF kinesthetic feedback for object shape discrimination while grasping virtual objects.

grasp sensations through wearable haptic devices necessitates feedback across multiple phalanges. Various wearable devices providing multi-phalangeal sensation for virtual object manipulation have been presented.

For delivering cutaneous feedback, prior work developed a glove for distinguishing 3D shapes by vibrotactile feedback [14] with reduced performance. Since proprioceptive cues strongly influence the perception of object shape and size [15], several wearable devices have been developed to deliver multi-phalanx kinesthetic feedback, such as linkage-based exoskeletons [16], [17], pneumatic gloves [18], and devices using reconfigurable materials [19]. However, grasp-based shape perception relies on the integration of both cutaneous and proprioceptive cues [2], [15], [20], rather than either modality alone. More recent approaches have introduced multi-phalanx and multimodal haptic gloves that combine these cues, such as a tendon-driven mechanism providing pressure on finger pads alongside multi-phalanx kinesthetic feedback [21], and devices using electrostatic clutches for multi-joint kinesthetic actuation with fingertip vibrotactile feedback [22]. Their approach enabled movement of individual joints and phalanges, and cutaneous sensation on the fingertips for a comprehensive VR object grasping experience. However, as a key limitation, bulky hardware or the use of high voltage may reduce wearability and comfort.

Most existing grasping devices deliver vibration only at the position where the vibration motor is attached. For efficiency, prior approaches have focused on collision-based fingertip-only tactile feedback, while overlooking the broader range of sensations experienced across the finger during natural grasping. An alternative and effective vibrotactile rendering method like phantom sensation [23], [24] has been developed for the smooth and continuous haptic experience. While several

H. Lee is with the KAIST Robotics Program, Daejeon, South Korea (e-mail: leeoh@kaist.ac.kr).

E. Kim and S. H. Yoon are with the KAIST Graduate School of Culture Technology, Daejeon, South Korea (e-mail: ehlkim0215@kaist.ac.kr; sangho@kaist.ac.kr).

R. Kim is with the KAIST School of Computing, Daejeon, South Korea (e-mail: rachel02@kaist.ac.kr).

Manuscript received November 22, 2025.

This paper was produced by the IEEE Publication Technology Group. They are in Piscataway, NJ.

studies have applied this phenomenon to generate localized or moving sensations along the fingers [25], [26], [27], no work except [28] has integrated phantom-based vibrotactile rendering with kinesthetic feedback. As kinesthetic feedback induces hand movements over certain durations, combining it with spatiotemporal vibrotactile cues may enhance kinesthetic perception or produce novel integrated haptic experiences. Moreover, the use of phantom sensations for 3D shape or surface perception remains underexplored. By generating perceived motion across a wider area with fewer actuators, phantom sensations offer potential for rendering complex shapes with appropriate algorithms.

In this paper, we propose VibGrasp, a novel haptic glove and multimodal rendering method, which enriches the sensation of grasping various shapes by delivering diverse vibration patterns across phalanges with 1-DOF kinesthetic feedback (Figure 1). We explore the differences in object shape recognition by reproducing the gradual tactile sensation from the proximal phalanx (PP) to the distal phalanx (DP) during hand flexion with the entire hand. The novel method exploits the human perceptual system’s ability to integrate proprioceptive information from hand movements with coordinated vibrotactile feedback [29] to create convincing illusions of different object shapes. The funneling illusion [23], also known as the phantom sensation [24], generates stationary or motion patterns by modulating the spatiotemporal dimension. We designed and developed an exoskeleton glove, which incorporates two haptic motors positioned above the dorsal side of the distal and proximal phalanges. These actuators transmit vibration through the structure and induce sensations on the ventral side of the finger.

We hypothesize that vibrotactile patterns differing in duration, stimulation area, and transition profiles can evoke the sensation of grasping different object shapes when combined with natural hand flexion. To examine this, two studies from Shape Perception Study investigate how various tactile patterns influence users’ shape selections. User Experience Study evaluates the user experience of our method in a VR grasping scenario compared to prior rendering techniques. Our main contributions are as follows:

- A novel haptic shape rendering approach that synchronizes multi-phalangeal spatiotemporal vibrotactile patterns with active kinesthetic feedback during hand flexion.
- Development of an exoskeleton glove with dual dorsal haptic motors to transmit vibration on the ventral finger surface.
- An analysis of user studies validating shape perception tendencies across haptic rendering patterns and evaluating user experience of our method.

II. RELATED WORKS

A. Vibrotactile Haptic Devices for Shape Perception

Cutaneous feedback on the ventral side of the finger plays a key role in shape discrimination by providing immediate tactile cues during object grasping [30]. Therefore, tactile haptic devices providing sensation on the finger, especially the fingertip, have been widely explored in prior works.

For example, FingerPrint by Zhakypov et al. [31], Lim et al. [32], and Prattichizzo et al. [33] applied directional forces to the fingertip using pneumatic actuation, shape memory alloys (SMA), and DC motors, enabling users to perceive object contours through slanted surface sensations. However, while effective for precision grasp, fingertip-based feedback is limited in representing whole-hand interaction.

To minimize hand obstruction while providing full hand feedback, wrist-mounted mid-air ultrasonic devices [34] and encounter-type devices [35], [36] have been explored, enabling greater freedom of movement. However, these approaches require consistent finger tracking to deliver stimulation at specific locations and additional end-effector mechanisms to render diverse haptic cues. Tanaka et al. [37] used electrostimulation to evoke full-hand tactile sensations with simple hardware, although such stimulation may introduce discomfort for some users. Instead, vibrotactile gloves provide a practical solution for delivering localized tactile cues with relatively simple hardware. Martínez et al. [14] designed the glove system for multi-phalangeal vibrotactile feedback, which enables users to distinguish object shapes during grasping. However, the lack of kinesthetic constraints increases mental workload and task completion time. In addition, these systems usually rely on collision-based triggering, applying brief vibrations at the fingertip or the position where the vibration motor is attached, as the hand collides.

In this work, we aim to enhance the effectiveness of multi-phalangeal vibrotactile feedback by actively rendering using a novel spatiotemporal rendering method with hand flexion, rather than relying solely on collision-based triggers.

B. Kinesthetic Finger Haptic Device for Shape Perception

The perception of the orientation and motion of one’s limbs and joints is referred to as proprioception [38]. Proprioceptive feedback plays a critical role in the discrimination of object shapes and sizes [15]. Concerning haptic representation, providing kinesthetic feedback to restrict finger movement at specific positions, or to guide the finger movement along object contours, is essential for tasks involving object shape discrimination. Various wearable devices have been developed to control hand movement, employing mechanisms such as pneumatic actuation [39], [40], wire-driven systems [9], [41], [10], [42], motor-driven systems [43], and using an electrostatic brake [44]. Although these devices provide efficient kinesthetic blocking during grasping, fingertip-focused feedback limits overall hand motion and the representation of detailed geometric features like edge and contours.

For the case of power grasp, all three finger joints are braked individually along with the object’s shape. More advanced devices capable of providing high degrees of freedom (DOF) and independent joint control have been introduced. These include mechanisms that control multiple phalanges via linkage control through tendon-driven or motor-driven mechanisms [16], [17], pneumatic actuators [18], and using reconfigurable materials [19]. These devices could control individual joint angles precisely, thereby achieving high-resolution hand movement and the intended hand pose.

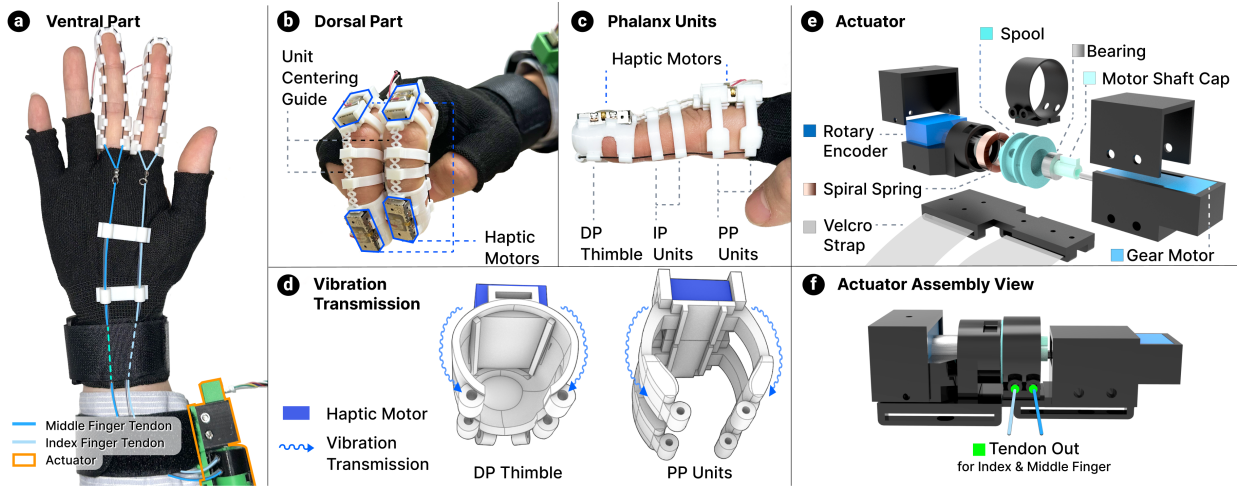


Fig. 2. The open-type exoskeleton glove for stable routing and efficient vibration transmission. (a) Ventral part and (b) Dorsal part of the glove. Two haptic motors are mounted at the DP thimble and the PP units. (c), (d) Side and Perspective view of finger units. (e), (f) Exploded and Assembly view of the actuator.

However, shape perception during grasping relies on the integration of both cutaneous and proprioceptive feedback from distinct sensory receptors [15], [20], [2], rather than on a single sensory modality. To achieve more realistic and immersive interactions, multimodal haptic devices have since been developed to combine cutaneous and kinesthetic feedback. For instance, EStatiG delivered an electrostatic brake to individual joints while providing vibrotactile feedback at the fingertips, enabling users to perform object shape recognition tasks with a high subjective rating [22]. In addition, Baik et al. [21] used a tendon-driven structure to control the metacarpophalangeal and interphalangeal joints independently, while also applying pressure feedback at the distal interphalangeal joint to simulate fingertip contact, thereby achieving a high subjective rating. Despite these advancements, such devices often remain bulky and heavy, require complex computation to support high-DOF control, and suffer from design complexity. Moreover, although multimodal feedback has been explored, multiphalangeal cutaneous feedback, along with the kinesthetic feedback, remains underexplored.

This paper investigates whether 1-DOF kinesthetic feedback can sufficiently allow users to perceive and discriminate different object shapes if provided in conjunction with vibrotactile patterns across multiple finger joints.

C. Vibrotactile Haptic Rendering

Previous vibrotactile haptic rendering methods for grasping virtual objects have primarily relied on collision-based triggers, delivering feedback only to the position where actuators are attached [45], [46]. However, during the grasping of real objects, cutaneous sensations are distributed across multiple phalanges. This requires not only activation beyond the specific locations where actuators are fixed, but also smooth and continuous vibration across the finger.

To achieve a wider activation range while maintaining a few actuators, researchers have developed an efficient haptic rendering method like phantom sensation [23], [24], [47]. Funneling effect, in other words, phantom sensation, provides

an illusory sensation between a few actuators, which can be both stationary or moving within that area [47], [48], [49]. The moving-like phantom sensation is widely referred to as “apparent haptic motion [50], [51].” Several applications of these phenomena were suggested to provide sensation across the digits [25], [26], [27]. Nevertheless, these approaches have typically been limited to static hand postures, where vibration patterns are rendered while the hand remains fixed. Therefore, Lee et al. [28] has investigated the application of phantom sensation-based vibrotactile patterns under kinesthetic feedback being actively provided. Also, the authors have explored this approach for object shape discrimination tasks.

Based on the rendering method suggested by [28], this work further advances the capabilities of employing various patterns created by using phantom sensation, while integrating it with 1-DOF kinesthetic feedback for shape perception. The novel method can sufficiently provide the sensation of a smooth and gradual sensation that the user can feel while slowly power-grasping the object, while maintaining a compact size and low energy consumption.

III. GLOVE DESIGN

An open-type exoskeleton glove providing flexion kinesthetic feedback along with vibrotactile feedback is designed (Figure 2). The glove incorporates four haptic motors (AFDU1A031A, Alps Alpine) and a tendon-driven kinesthetic haptic module. We used Teensy 3.5 as a microcontroller, and two TDA2822 dual-channel stereoscopic audio amplifier modules (ELB060304, YwRobot) to operate two haptic motors. H-bridge motor driver (2A L298N, SMG) precisely controlled a micro metal gearmotor (#5227, Pololu), which generates $5.0 \text{ kg} \cdot \text{cm}$ of stall torque at 0.75 A and 12 VDC .

The glove consists of two finger modules, a fabric glove that covers the palm, and the actuator. The glove is designed to enable finger flexion through anchor routing, leaving the ventral side of the finger open to preserve natural tactile sensation (Figure 2 (a)). The haptic motors are placed on the dorsal side of the finger to allow unobstructed hand

movement. A tendon routing design from the fingertip to the metacarpophalangeal joint presented in prior work [52] is adopted. Tendons of each finger pass all the anchors of each finger module and are connected to the spool through the tendon sheath. A Teflon tube with an inner diameter of 1.5 mm was used as the tendon sheath [53] to transmit the force with minimized friction. In addition, the velcro strap on the wrist firmly fixes the glove to prevent it from shifting when the tendon is pulled, and to increase the stability of actuation. The glove and wrist-worn actuator weigh 100.4 g (58.2 g for the actuator), and the control circuit with its housing weighs 142 g, resulting in a total weight of 242.4 g.

A. Finger Modules

As described in Figure 2 (b), and (c), a single finger module consists of five phalanx units, including two proximal phalanx (PP) units, two interproximal phalanx (IP) units, and one distal phalanx (DP) thimble, along with a unit centering guide that aligns and connects all phalanx units. All phalanx units are 3D printed using Polylactic Acid (PLA). Anchors positioned at the end of each open ring and the underside of the thimble guide the tendon along a designated path as illustrated in Figure 2 (a), ensuring it is pulled downward.

To initiate vibrotactile feedback, two haptic motors are mounted at the upper side of the PP units and the DP thimble. As we aimed to provide phantom vibration on the IP, no motor was attached to the IP units. Our design enables vibration to be transmitted through the PP units and DP thimble, allowing perception on the ventral surface of the fingertip while keeping the skin unobstructed. According to the prior work, referred phantom sensation suggests that low-frequency stimuli (104 - 133 Hz) applied to areas with fewer mechanoreceptors can be perceived at adjacent regions with denser mechanoreceptor distributions [54]. In addition, prior work demonstrated that vibration around 122 Hz delivered to the finger's lateral region propagates structurally toward the finger pad [55], [56], and also perceptually reported as being felt at the finger pad [57].

Building on these, we designed PP units and a DP thimble that promote vibration perception at the finger pad as described in Figure 2 (d). We combined limited dorsal contact, enhanced vibration transmission to the lateral and ventral side, and the perceptual effect of referred phantom sensation. A 0.8 mm silicone-covered bridge at the inner top of the units reduces dorsal contact and dampens vibration. The PP and DP units wrap firmly around the lateral side of the finger to promote efficient vibration transmission. The overall geometry follows a secure finger-mounting design from prior works [52], [58], [59], but we widened PP units around the lateral area to increase contact area. The DP thimble includes an open region to match the contact area of the PP units. The motors are driven at approximately 122 Hz to induce deformation toward the finger pad in accordance with prior findings [55].

The unit centering guide, which is 3D-printed with Thermo-plastic Polyurethane (TPU), is designed in a honeycomb pattern to enable elongation as the finger flexes. Each honeycomb cell has a size of 5 mm x 2.5 mm ($\varnothing = 0.8$ mm). The guide passes through the upper holes of the phalanx units, which

are designed to be 1 mm narrower than the guide, thereby securing each unit in place. This ensures that the routing units remain fixed in their designated positions for different hand sizes and prevents unintended movement. For the experiment, we prepared three sizes (small, medium, and large) to ensure proper fit across different hand sizes.

B. Force Feedback Actuator for Fingers

The kinesthetic feedback actuator, comprising a gear motor and a spool with a torsional spiral spring, is designed (Figure 2 (e),(f)). The actuator can be firmly mounted on the user's arm by two Velcro straps under the module. It has overall dimensions of approximately 9 cm x 2 cm x 2.5 cm, while the tendon spool exhibits diameters of 18 mm (index) and 16 mm (middle finger). When haptic rendering is activated and the motor operates, a protrusion on the motor shaft cap pushes the protrusion inside the spool, inducing spool rotation and finger flexion. The torsional spiral spring connected to the spool prevents tendon slack [10]. A 1024-PPR rotary encoder (EMS22A50-M25-LD6, Bourns Inc.), mechanically coupled to the spool, allows the real-time tracking of the hand flexion. The required speed of 0.112 RPM is achieved through the PID control. The index and middle finger tendons that exit from the spool are connected to the respective fingers.

IV. HAPTIC RENDERING PATTERN DESIGN

We hypothesized that vibrotactile patterns with different spatiotemporal properties would significantly influence object shape discrimination when flexion trajectory and final hand posture were held constant. To examine this, five vibrotactile patterns with different spatiotemporal profiles are designed for Study 1 from Shape Perception Study, and three vibrotactile patterns with different transition profiles of the apparent haptic motion for Study 2 (Figure 3). Those patterns are provided along with kinesthetic feedback simultaneously. We aim to provide a shape-like sensation mainly through the vibration pattern. The role of kinesthetic feedback is to ensure that vibrotactile patterns are consistently delivered with the same flexion progression per activation.

A. Active Kinesthetic Feedback Design

The active kinesthetic feedback for flexion is identically provided in every activation. The flexion is designed to start from a flat hand and end when the DP reaches the start of the PP phalanx, to represent a grasping-like hand shape. We preliminarily recorded the rotary encoder value of each user when the hand was flat and when the DP arrived at the target. This calibration allows participants to perceive the vibration at the same proportional point in the motion process. The motor stops once the target rotary encoder value is reached. The total time taken is labeled as the flexion duration in Figure 3.

B. Vibrotactile Patterns for Primitive Shape Perception Study

To generate vibration patterns with different durations and area, algorithms of 1D stationary phantom sensation [48] and 1D apparent haptic motion [49] are adopted.

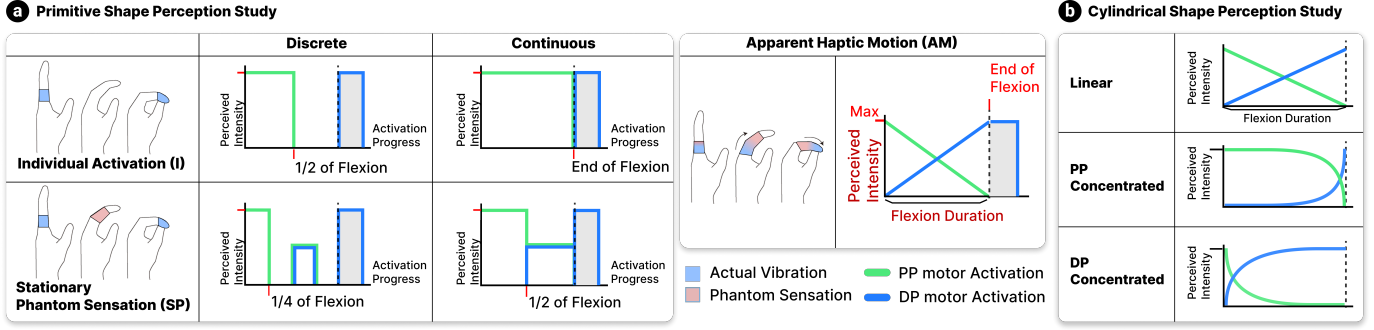


Fig. 3. Haptic rendering patterns for the Shape Perception Study, Study 1 and 2. (a) Vibrotactile pattern design varying the positional dimension, including Individual activation (I), activation with Stationary phantom sensation (SP), and activation with Apparent haptic motion (AM). (b) Three vibrotactile patterns using apparent haptic motion with different transition profiles to modulate the concentration of vibration on phalanges.

1) *Rendering Equation*: The 1D stationary phantom sensation is generated by adjusting the relative amplitudes of two haptic motors on the DP and PP, creating an interpolated tactile stimulus on the IP. Intensity calibration is required to ensure perceptual consistency of the vibration amplitude with the proximal (A_{PP}) and distal (A_{DP}) phalanges due to differences in mechanoreceptor density [30], [60]. To establish a perceptual reference, the PP haptic motor is driven at its maximum intensity, denoted as A_{ref} . The intensity of the DP haptic motor is then calibrated to produce a perceived vibration that matches the reference. A perceptual compensation factor α is empirically determined such that the amplitude of the DP actuator is continuously scaled to match the perceived intensity of the PP actuator, according to the relationship $A_{DP} = \alpha A_{PP}$. Here, the vibration amplitude is calculated as Equation 1:

$$A_i = A_{ref} \left(1 - \frac{d_i}{D} \right) \quad (1)$$

where A_i is the amplitude of vibration, d_i is the distance from vibration motor i to the target location, and D is the total distance between actuators. The vibration duration is adjusted to control the duration of each stimulus to generate multiple tactile patterns.

For the 1D apparent haptic motion, the linear transition of perceived vibration from the PP to the DP over time is created for Study 1. The actuator amplitudes are defined by:

$$A_{PP}(t) = A_{ref} \left(1 - \frac{t}{T} \right), \quad A_{DP}(t) = A_{ref} \left(\frac{t}{T} \right) \quad (2)$$

where T is the total transition duration. To ensure perceptual consistency, the same intensity correction is applied only at $t = 0$, allowing the linear transition to proceed naturally.

2) *Vibrotactile Pattern Design*: We followed the pattern design that was adopted in our prior research [28]. Figure 3 illustrates the haptic patterns for Study 1. Three primary vibration patterns were established based on the vibration area: individual point activation (Individual), activation with 1D stationary phantom sensation (SP), and activation with 1D apparent haptic motion (AM). The Individual pattern activates the PP and DP separately. The SP pattern induces phantom sensations at the IP so that users can perceive distinct sensations in the sequence of PP, IP, and DP. The AM pattern creates a dynamic phantom sensation of simulating a shifting

vibration from PP to DP [47] linearly. Overall, the PP motor activates at the start of the flexion, while DP always vibrates at the end of the flexion. The IP vibration triggers at the midpoint of the target rotary encoder value. We provided sinusoidal vibration with a frequency of 122 Hz [55].

Next, we divided the Individual and SP patterns into Discrete and Continuous subcategories based on vibration continuity. Discrete patterns include pauses between vibrations, while Continuous patterns deliver individual vibrations to each phalanx sequentially without any break. To summarize, vibrotactile patterns including Individual-Discrete (I-Discrete), Individual-Continuous (I-Continuous), Stationary-Discrete (SP-Discrete), Stationary-Continuous (SP-Continuous), and Apparent Motion (AM), were utilized in Study 1. Along with the flexion, the vibration starts when the rotary encoder reaches a certain value and lasts for a certain duration. Overall, each pattern was designed using a fixed five-stage duration, while the ratio between vibration and break within these stages varied across conditions.

C. Haptic Patterns for Cylindrical Shape Perception Study

To examine whether the transition profile between the two actuators influences the perception of different cylindrical shapes, we modulated the 1D apparent haptic motion to make linear, DP Concentrated, and PP Concentrated profiles.

To generate non-linear transition profiles between the PP and DP actuators, we employed a power-law function that produces either an early or late increase of vibration intensity depending on the direction of the transition. By applying the power-law term $(t/T)^\beta$ and its time-reversed counterpart $1 - (1 - t/T)^\beta$, we created two distinct profiles: PP concentrated transitions, where the perceived high intensity remains longer near PP before shifting to the DP actuator, and DP concentrated transitions, where the high intensity remains longer near the DP actuator. We empirically selected the exponent $\beta = 6$ to achieve a perceptually salient yet smooth transition between the PP and DP actuators. The actuator amplitudes for PP Concentrated profile are defined by:

$$A_{PP}(t) = A_{ref} \left[1 - \left(\frac{t}{T} \right)^\beta \right], \quad A_{DP}(t) = A_{ref} \left(\frac{t}{T} \right)^\beta, \quad (3)$$

Shape Perception Study

Study 1 & 2 : Primitive Shape Perception & Cylindrical Shape Perception

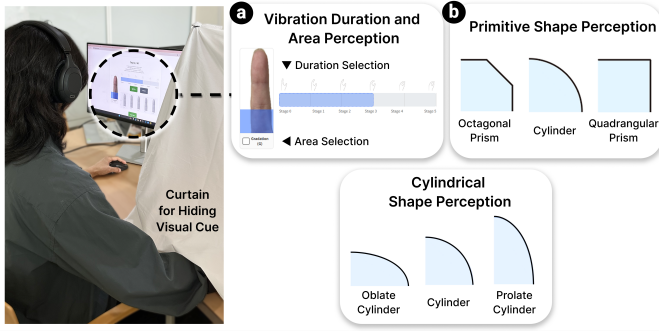


Fig. 4. Study 1 & 2 setups. (a) Perceived vibration duration and area selection task and (b) Primitive Shape perception task (Cylinder, Octagonal Prism, and Quadrangular Prism) were conducted for Study 1. Study 2 collected cylindrical shape perception tendencies : oblate, original, and prolate cylinders.

and the actuator amplitudes for DP Concentrated profile are defined by:

$$A_{DP}(t) = A_{ref} \left[1 - \left(1 - \frac{t}{T} \right)^\beta \right], \quad (4)$$

$$A_{PP}(t) = A_{ref} \left(1 - \frac{t}{T} \right)^\beta.$$

The Figure 3 illustrates the 3 patterns for cylindrical shape perception studies.

V. SHAPE PERCEPTION STUDY

Shape Perception Study aims to investigate how spatiotemporal vibrotactile patterns along with kinesthetic feedback influence participants' perception of object shapes.

In the first study, three primitive shapes were provided to evaluate whether specific haptic patterns converged toward particular shapes. Next, our previous work evaluated that apparent haptic motion provided with kinesthetic feedback tended to be perceived as grasping a curved surface [28]. Therefore, we altered the transition profile of AM and provided three patterns in the second study. We offered three different cylindrical surfaces as options to determine whether each distinct haptic motion transition profile converged to a specific elliptical shape. The study was approved by the Institutional Review Board (KAISTIRB-2025-124).

A. Study 1 : Primitive Shape Perception Study

During the Study 1, the tendency to select three different shapes under five different haptic patterns was analyzed. In addition, participants' responses regarding the timing and location of perceived vibrations were collected to determine how the interaction between proprioception of hand movement and vibration affects the identification of stimulated locations.

1) *Design & Procedure*: We recruited 18 right-handed participants (9 men, 9 women; $M = 26.67$ years, $SD = 3.69$). Study 1 consisted of two within-subject experiments (Figure 4). All participants completed the perceived vibration duration/ area selection task followed by the shape selection

task. In each experiment, the five haptic patterns (Figure 3 (a)) were presented once per repetition across five repetitions, with the order randomly selected from the possible permutations of the five conditions. Each participant experienced five distinct permutations of conditions. Both tasks began with five training trials followed by 20 experimental trials. Participants were informed that the kinesthetic feedback would remain identical across conditions, while the accompanying vibrotactile patterns would vary.

We first explained the study's purpose and calibrated the glove's kinesthetic and vibrotactile parameters. Vibrotactile intensities were calibrated to ensure consistent perception between PP and DP. Participants then confirmed their ability to distinguish vibrations at three phalanges. They were instructed to imagine grasping the object slowly, making contact from the right side to the top. During the first task, participants identified the moments of perceived vibration across five hand-flexion stages and indicated the phalanges where vibration was felt. Multiple phalanx selections were allowed, and a "Gradation" option was provided for gradually shifting sensations. In the subsequent shape-selection task, participants chose among an Octagonal Prism, a Cylinder, and a Quadrangular Prism, selected based on the power-grasp taxonomy [61]. White noise and a curtain prevented inference from auditory or visual cues. After completing both tasks, we conducted a brief interview to collect qualitative insights on shape-selection strategies. Also, participants identified the location of perceived vibration (ventral, dorsal, lateral sides, or whole finger) to verify vibration transmission to the ventral side.

2) *Result 1 : Vibration Duration and Area Perception*:

Three participants were excluded because they reported relying on kinesthetic cues rather than vibration to judge object shape. We summarized the vibrated area reported at each flexion stage and converted it into percentage distributions. Figure 5 shows a heatmap of the percentage distribution for all area-stage combinations. Each column sums to 100%, and red-outlined cells indicate the blocks where vibration was actually delivered. The y-axis lists all possible phalanx selections including the actually activated area (PP, PP-IP, IP, IP-DP, DP), "No" for no vibration (break), and responses considered as errors such as "DP-PP" or "All" (perceiving vibration across all phalanges simultaneously at a single stage). When a gradation was selected, we interpolated between the first and last reported phalanges according to the number of stages. For example, gradation from PP, IP, to DP across five stages was mapped to PP, PP-IP, IP, IP-DP, and DP; a gradation from PP to IP across four stages was mapped to PP, PP-IP, PP-IP, and IP. As we instructed that all experimental patterns were designed to progress from PP toward DP, "Gradation" responses were always mapped from proximal to distal.

Participants' most frequent responses at each stage closely followed the actual activation area-stage blocks in the I-Discrete, AM, and SP-Discrete patterns. In these patterns, participants predominantly reported vibration at the phalanx that matched the stimulation actually delivered at each stage. The SP-Discrete pattern showed the highest correspondence, with accuracy rates ranging from 68.3% to 81.7%. In contrast, the I-Continuous pattern showed markedly poor correspondence: no

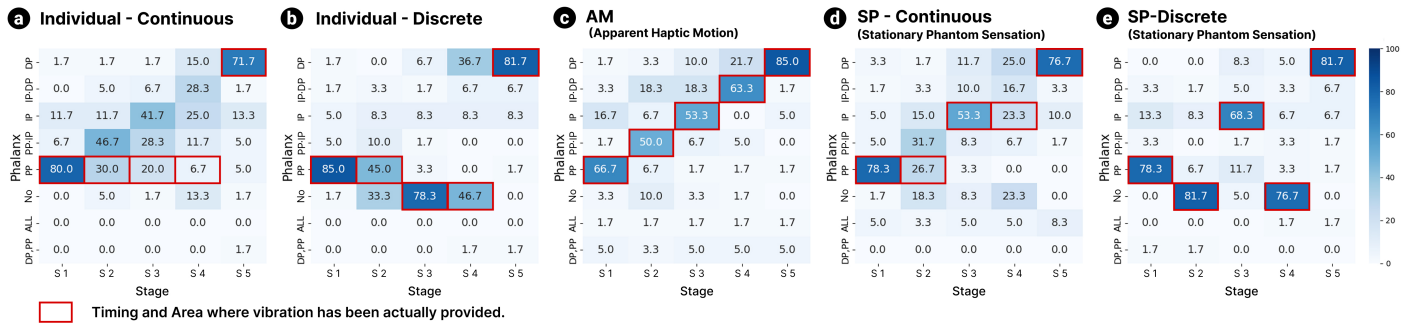


Fig. 5. Heatmap of the vibration perception percentage at phalanges per hand flexion stages across five haptic patterns. The red square indicates the actual timing and area where the vibration has been provided.

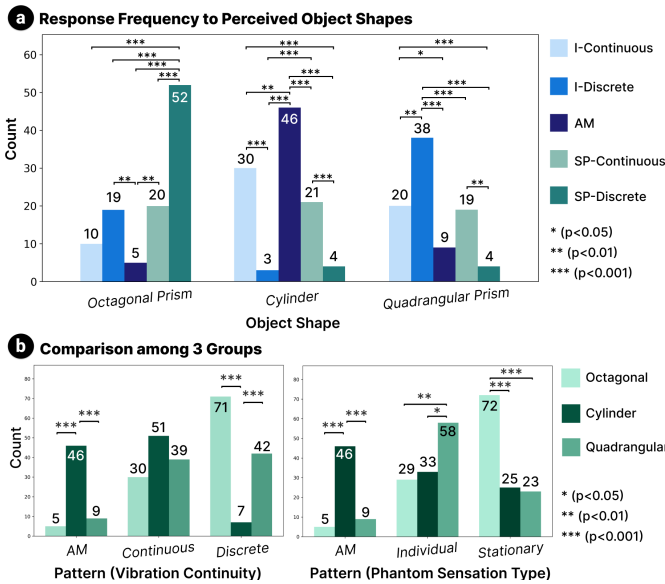


Fig. 6. The response frequency of five different haptic feedback renderings for associating three object shapes.

intermediate block between the first and last stages exceeded 30% accuracy. The blocks with the highest answer rate at each stage show the trend to shift gradually upward from PP toward DP, even though vibration was provided only at PP. A similar upward-shift bias was observed in the SP-Continuous pattern, where the highest reported phalanx at each stage tends to be more distal than the actual activated phalanx.

Across patterns where vibration was intended at the IP, the accuracy of the IP was generally lower than the PP and DP. This aligns with the interview, in which 13 of 18 participants reported difficulty precisely discriminating IP vibration. The result is also attributable to the fact that IP stimulation was rendered via phantom sensations rather than direct actuation.

3) *Result 2 : Primitive Shape Perception:* We analyzed 15 participants’ shape selection behavior by performing a frequency analysis and conducting pairwise Chi-Square tests with Bonferroni-adjusted p-values. The graph of the frequency analysis result is shown in Figure 6. A chi-square analysis revealed a strong relationship between pattern type and object shape selection ($\chi^2(8) = 164.63, p < .001$). Bonferroni-corrected pairwise comparisons revealed distinct tendencies in

object-shape selection across the different vibrotactile patterns. The SP–Discrete pattern yielded significantly higher selections of Octagonal prism compared to all other patterns ($p < .001$). For the Cylinder, the AM pattern showed a higher tendency to choose it compared to the other conditions (I-Discrete, SP-Discrete, SP-Continuous : $p < .001$, I-Continuous : $p = .005$). For the Quadrangular prism, I–Discrete pattern exhibited a significantly higher selection rate relative to other patterns (AM, SP-Discrete, SP-Continuous : $p < .001$, I-Continuous : $p = .002$).

Additional analyses were conducted by regrouping the patterns according to vibration continuity and funneling type. Within the same phantom sensation type, perceptual outcomes significantly differed: Apparent haptic motion strongly increased cylinder selections ($p < .001$), No phantom sensation increased quadrangular prism selections ($p < .01$), and Stationary Phantom sensation increased octagonal-prism selections ($p < .001$). Within the same vibration-continuity group, Discrete patterns produced significantly higher selections of quadrangular or octagonal prisms (both $p < .001$), whereas Continuous patterns showed no significant differences across the three shapes. Overall, the findings support the hypothesis that spatiotemporal differences in vibrotactile cues directly shape the perceived object geometry.

B. Study 2 : Cylindrical Shape Perception Study

Study 2 investigated whether participants could discriminate cylindrical shapes based on different apparent haptic motion transition profiles, evaluating the tendency to select specific cylindrical shapes under different haptic patterns.

1) *Design & Procedure:* Three haptic patterns, which are Linear, PP Concentrated, and DP Concentrated patterns, were provided in a randomized order with five repetitions, for a total of 15 trials. The same participants from Study 1 took part in this experiment. Participants selected one of three cylindrical shapes which are a prolate cylinder, a cylinder, or an oblate cylinder. Before the study, we presented a baseline stimulus, which is a linear transition profile of the apparent haptic motion. Participants were instructed to choose the shape that best matched their perception, and to select the normal cylinder if they were unable to discriminate among the options. A brief interview was conducted to gather their reason for each selection. White noise and a curtain were used to reduce

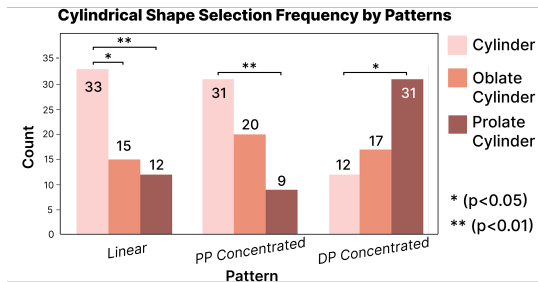


Fig. 7. The response frequency of three different transition profiles of apparent haptic motion pattern (AM) for associating three cylindrical shapes.

auditory and visual cues. Participants were also informed that only the vibrotactile patterns varied across conditions, while the kinesthetic feedback remained constant.

2) *Result*: 15 participants’ data were used for analysis due to the same reason as in Study 1. A chi-square test of independence found a significant relationship between pattern type and shape selection ($\chi^2(4) = 27.76, p < .001$). Bonferroni-corrected pairwise comparisons revealed distinct tendencies for each pattern (Figure 7. For the Linear pattern, participants selected the normal cylinder significantly more often than both the prolate ($p = .005$) and oblate ($p = .028$) cylinders. For the PP Concentrated pattern, only the contrast between the prolate and normal cylinder reached significance ($p = .002$), with the normal cylinder being chosen most frequently. For the DP Concentrated pattern, participants showed a significantly higher tendency to select the prolate cylinder compared with the normal cylinder ($p = .011$), and oblate selections followed prolate selections in frequency. Overall, the Linear pattern showed the strongest preference for the baseline cylinder. The PP Concentrated pattern led participants to choose the baseline cylinder most frequently as well. Although not statistically significant, participants showed a slightly higher preference for oblate over prolate shapes. In contrast, the DP Concentrated pattern induced a tendency toward the prolate shape.

VI. USER EXPERIENCE STUDY

User Experience Study evaluated our novel active haptic-rendering method and device by comparing it with three haptic methods and devices from prior works to assess user experience during VR grasping. Based on the Shape Perception Study which revealed shape selection tendencies associated with specific vibration patterns, we hypothesized that the our rendering method (VibGrasp) would offer enhanced effectiveness in both object shape identification and user experience during object manipulation in VR. To compare with VibGrasp, the three conditions for comparison were prepared: (1) Three phalanges passive kinesthetic condition (Kin), applying resistance to the contacted phalanges; (2) Two phalanges passive vibration condition (Vib), delivering vibration to the PP and DP upon collision; and (3) Combined three phalanges passive kinesthetic + two phalanges vibration condition (Kin+Vib), providing both resistance and vibration.

To render passive kinesthetic feedback at all three phalanges, we built a glove for the experiment with dorsal

User Experience Study

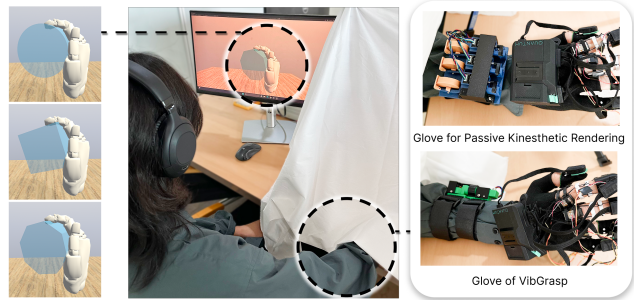


Fig. 8. User Experience Study setups. Four haptic conditions, including VibGrasp rendering method, were compared grasping three virtual objects.

routing anchors and tendons attached to the PP, IP, and DP units (Figure 8). Tendon extension was controlled by custom actuators using three micro gearmotors (Pololu #5227). Before contact, tendons could move freely. Upon collision, a rotating protrusion on each motor’s shaft blocked tendon motion, generating passive resistance to respective phalanges. Vibrotactile motors at PP and DP provided localized vibration without inducing phantom sensations at IP. A Manus hand-tracking module (Quantum Gloves, Manus Meta) was mounted dorsally, and visual and auditory cues were blocked.

A. Study Design & Procedure

A within-subject experiment was conducted in which all participants experienced four haptic-rendering conditions: Kin, Vib, Kin+Vib, and VibGrasp. Seventeen right-handed participants (8 men, 9 women; $M = 25.88$ years, $SD = 2.66$) were recruited. Different actuator modules were used for each condition: a three-motor kinesthetic module for Kin and Kin+Vib, our lightweight active actuator for VibGrasp, and no kinesthetic module for Vib. Actuator modules were physically exchanged between conditions by the experimenter. A Unity scene was designed to display a hand grasping the same three objects used in the Shape Perception Study. The virtual hand was anchored at the wrist near the object.

The passive and active conditions operated through different interaction mechanisms. For the comparison conditions which all operate in a passive way, participants moved their hands freely and received haptic feedback only during collisions between the virtual hand and object. In contrast, for VibGrasp, the hand automatically flexed and delivered predetermined haptic feedback upon entering a predefined interaction region. Based on findings from the Shape Perception Study, I-Discrete feedback was assigned to the Quadrangular Prism, SP-Discrete to the Octagonal Prism, and AM to the Cylinder. After feedback delivery, the motors rewound the tendons to restore free movement.

The haptic conditions were presented in a randomized order. After grasping all three objects, participants rated their VR haptic experience across five categories (Realism, Immersion, Satisfaction, Comfort, and Harmony [10], [28], [62]) using a 7-point Likert scale. Participants could revisit any condition and revise previous responses as the study progressed.

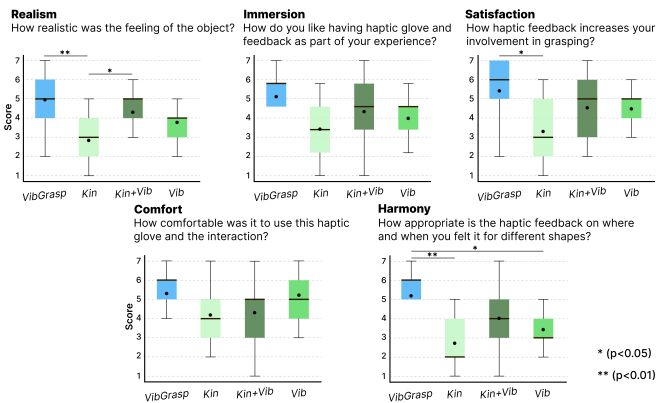


Fig. 9. Result of User Experience Study. Five subjective rating categories (Realism, Immersion, Satisfaction, Comfort, and Harmony) are compared.

B. Result

We conducted a Friedman Test across the four haptic conditions, followed by Wilcoxon signed-rank tests for post hoc pairwise comparison. The graph of the result is described in Figure 9. We found a significant effect of the condition for Realism ($\chi^2(2) = 16.29, p = .001$), Immersion ($\chi^2(2) = 9.16, p = .027$), Satisfaction ($\chi^2(2) = 9.26, p = .026$), and Harmony ($\chi^2(2) = 15.11, p = .002$). For Comfort, no significant difference was found among the four conditions.

The following post hoc Wilcoxon signed-rank test with Bonferroni correction revealed significant pairwise differences across conditions. For Realism, we found significant differences between VibGrasp and Kin ($p = .007$) and between Kin+Vib and Kin ($p = .020$). For Satisfaction, a significant difference was found between VibGrasp and Kin ($p = .016$). For Harmony, VibGrasp showed a significant difference between Kin ($p = .010$) and Vib ($p = .023$). No significant differences were observed for Immersion after the correction. In 3 out of 5 categories, VibGrasp outperformed the Kin condition. No conditions showed a significant difference between VibGrasp and Kin+Vib.

VII. DISCUSSION

A. Shape Selection in Relation to Haptic Pattern Perception

In Study 1 from the Shape Perception Study, we examined how different haptic feedback patterns influence shape perception during grasping, and found clear selection tendencies. SP-Discrete was associated with the Octagonal Prism, AM and I-Continuous patterns with the Cylinder, and the I-Discrete pattern with the Quadrangular Prism. Interview responses also supported these trends. Particularly, all participants reported that the sensation of continuous vibration moving across all phalanges led them to choose the Cylinder. Eleven participants reported perceiving the clear sensation on individual phalanges and the shift across them led to identification of angular shapes. To differentiate the Quadrangular and Octagonal Prisms, some participants used the number of perceived breaks, interpreting one break as the Quadrangular Prism and two as the Octagonal Prism. Others mentioned that they distinguished the Octagonal Prism when they felt

a clear sensation, specifically at the IP. These results indicate that participants used both the number of discontinuities and phalanx-specific cues to judge shape, suggesting future work to explore more influential cue types. In addition, we [28] found that participants preferred continuous patterns when visual cues were present in VR, as visual information amplifies tactile perception [63], [64], making discrete patterns feel comparatively awkward. To preserve the natural sensation of continuous patterns while improving their discriminability, future work could evaluate a minimal break duration that users can reliably perceive as distinct shapes.

We also investigated how the perceived vibrated area and timing related to participants' shape selections. Patterns that matched our intended perception in Study 1 showed a clear tendency toward specific shape selections. For the I-Continuous, the highest vibration perception percentage at each stage showed a gradual shifting trend, moving distally between PP and DP despite no activation in that area. This result aligns with the result from [28], which interpreted based on the sensory integration model [65]. Human perception assigns weights to sensory inputs based on their reliability. Prior studies also have shown that hand posture affects the perception of tactile stimuli [29], [66], indicating that tactile perception is not absolute when integrated with proprioceptive information. In our case, the stable and reliable proprioceptive cues from kinesthetic feedback may have overshadowed the more dynamic and less reliable vibrotactile cues, biasing the perceived area toward the more flexed phalanx. This proprioceptive dominance likely contributed to participants' tendency to perceive the vibration as following a curved trajectory, which may explain the preference for curved surfaces over angled shapes under the I-Continuous pattern. Future research on the phantom sensation algorithm regarding kinesthetic variables should account for sensory error and provide feedback at the exact intended position while flexing the hand. Further investigation could also include stimuli with varying motion directions and lengths to better evaluate spatial localization performance.

B. Cylindrical Shape Rendering

Post-study interviews were conducted to investigate the tendency to select the cylindrical shape observed in Study 2. Nine participants reported difficulty distinguishing the PP Concentrated pattern from the Linear pattern. Consistent with Study 1, sustained stimulation at PP was perceived as traveling distally during hand flexion, likely due to sensory integration with forward-moving kinesthetic cues [28]. Consequently, participants often misinterpreted the PP pattern as Linear and selected the normal cylinder more frequently.

For the DP Concentrated pattern, twelve participants reported that it produced a clearly distinguishable sensation focused on DP, and the study results showed a strong preference for the prolate cylinder. Six participants mentioned that the resistance felt at the fingertip when the finger was only slightly flexed gave the impression of touching a wall, which led them to select the prolate cylinder. However, five participants reported that prolonged vibration at the fingertip gave the

impression of prolonged contact with the top. This produced a sensation of touching the extended top surface, leading them to select the oblate cylinder. This contrary interpretation explains the reason for the lack of a significant difference between a prolate and an oblate cylinder.

Taken together, these findings suggest several practical guidelines for rendering cylindrical shape via VibGrasp for VR interaction. The Linear pattern would be appropriate for rendering a cylinder effectively, both with and without visual cues, as participants reliably distinguished it. To render a prolate cylinder, the DP Concentrated pattern appears most suitable. However, effective perception requires that finger flexion, visual cues of grasping the shape, and the timing of vibrotactile transitions be synchronized and delivered simultaneously.

C. Comparison of User Experience in VR

Overall, the User Experience Study showed that the Kin condition received the lowest mean scores across all metrics. Three participants reported difficulty perceiving passive kinesthetic feedback during object collisions in the Kin and Kin+Vib conditions. We observed that when tendon unwinding was blocked, some participants extended their fingers backward at the MCP joint and flexed within the shortened tendon range, reducing the perceived resistance at the phalanges. One participant also noted that the braking force applied to the dorsal side of the finger reduced realism in the Kin and Kin+Vib. In contrast, VibGrasp rendering method allows full finger flexion, stopping at the exact position, with sufficient tactile feedback, leading participants to perceive a more natural grasp. The result also indicates that the tactile cue plays a critical role in the sensation of grasping.

Comfort showed no significant differences across conditions, partly because the hand tracking device itself introduced weight and discomfort, as three participants mentioned. However, the other three participants indicated increased comfort with VibGrasp due to its lighter actuator (58.2 g) compared to the three motor comparison module (134.8 g). This suggests that comparable or improved performance and usability can be achieved with lower device weight and computational demand. Future work could further evaluate usability using less intrusive vision based hand tracking methods [67].

Harmony showed the largest mean score differences, with significant differences between VibGrasp and the two single-modality conditions. Four participants found VibGrasp easiest for shape discrimination due to shape-specific haptic patterns rather than collision-based feedback, while three reported lower scores due to constrained finger movement from predefined actuation. These results suggest that VibGrasp is suitable for scenarios that require accurate shape discrimination or limited visual information, such as hand occlusion. Future work should explore adaptive actuation or hybrid approaches with collision-based passive haptics.

D. Glove Design and Vibration Transmission

We developed a lightweight hardware system that combines 1-DoF kinesthetic feedback with a minimal number of

vibrators to deliver multi-location tactile cues during grasping. Compared to conventional linkage-based exoskeletons or wrist-mounted devices, the system is lighter and allows greater freedom of finger movement while also providing rich multimodal sensations. Placing the vibrators on the dorsal side of the fingers keeps the finger pad unobstructed, enabling more natural interaction with both real and virtual objects, potentially improving practicality for everyday VR interactions. However, the exoskeleton may cause occlusion in vision-based hand tracking when the dorsal side faces the camera, requiring additional pose sensing. In addition, the 3D-printed structure can introduce extra weight and discomfort. Future work would address these limitations by integrating compact pose sensors or exploring softer, transparent materials for the exoskeleton.

For vibration transmission, 14 of 18 participants (including those excluded from the Shape Perception Study) perceived vibration on the ventral side of the finger, indicating effective transmission to the intended region. However, three reported dorsal-side perception, and one reported lateral perception. These variations were mainly due to hand-size differences, as some participants did not fit the available glove sizes precisely, resulting in insufficient lateral contact. Compared with the inconsistent transmission on the lateral side, the dorsal side consistently remained in contact because of gravity and the reaction force produced as the tendon pulls the module inward during the flexion. This likely contributed to the dorsal perception by several participants. Future hardware improvements should ensure reliable transmission across different hand sizes. Vibration-damping structures could reduce unintended dorsal transmission, while mechanisms stabilizing ventral contact, such as torsion-spring-based structures, may improve fit. Incorporating thumb actuation would also be beneficial, given its key role in perceiving object shapes and sizes [11].

E. Future Works

To further demonstrate the adaptability of VibGrasp system across diverse grasping scenarios, future work would evaluate a broader range of object shapes, including asymmetric and irregular forms. Exploring additional rendering parameters, such as kinesthetic feedback length and force, as well as vibration duration, location, and amplitude, could enable richer reproduction of diverse object shapes. An adaptive rendering framework that adjusts these parameters based on detected object geometry could support teleoperation scenarios where shapes identified by a robot hand are conveyed to the user. Integrating robot-side sensing (e.g., grasp position and contact state) with user-side sensing, such as an FSR on the dorsal side of the thimble [68] to detect finger extension intent and transmit user commands to the robot, would enable intention-aware closed-loop control for realistic grasping interactions. Lastly, future studies with more participants may provide greater statistical power and reveal significant effects.

VIII. CONCLUSION

We propose a novel haptic shape rendering method and a glove that enhances shape perception during grasping by varying spatiotemporal vibration parameters through the

phantom sensation, providing with 1-DOF kinesthetic flexion feedback. The User Study results indicate that participants tend to associate Continuous and Apparent Motion patterns with Cylindrical perceptions, whereas Discrete patterns were perceived as angled shapes. Also, participants tend to perceive the Linear AM pattern as the cylinder, while DP Concentrated AM pattern as the prolate cylinder. In VR, VibGrasp showed higher subjective ratings for some categories of the user experience compared to prior methods. This work emphasizes the potential for better providing the sensation of diverse object shapes, enhancing interaction in VR for various applications.

ACKNOWLEDGMENTS

This work was supported by Electronics and Telecommunications Research Institute (ETRI) grant funded by the Korean government [26ZC1100, Development of Spatial Media Technology and Interaction Technology for Convergence of the Real and Virtual World].

REFERENCES

- [1] K. Minamizawa, D. Prattichizzo, and S. Tachi, "Simplified design of haptic display by extending one-point kinesthetic feedback to multipoint tactile feedback," in *2010 IEEE Haptics Symposium*. IEEE, 2010, pp. 257–260.
- [2] C. Pacchierotti, F. Chinello, M. Malvezzi, L. Meli, and D. Prattichizzo, "Two finger grasping simulation with cutaneous and kinesthetic force feedback," in *Haptics: Perception, Devices, Mobility, and Communication: International Conference, EuroHaptics 2012, Tampere, Finland, June 13-15, 2012. Proceedings, Part I*. Springer, 2012, pp. 373–382.
- [3] A. Girard, M. Marchal, F. Gosselin, A. Chabrier, F. Louveau, and A. Lécuyer, "Haptip: Displaying haptic shear forces at the fingertips for multi-finger interaction in virtual environments," *Frontiers in ICT*, vol. 3, p. 6, 2016.
- [4] L.-T. Cheng, R. Kazman, and J. Robinson, "Vibrotactile feedback in delicate virtual reality operations," in *Proceedings of the Fourth ACM International Conference on Multimedia*, 1997, pp. 243–251.
- [5] H. Liu, Z. Zhang, X. Xie, Y. Zhu, Y. Liu, Y. Wang, and S.-C. Zhu, "High-fidelity grasping in virtual reality using a glove-based system," in *2019 IEEE International Conference on Robotics and Automation (ICRA)*. IEEE, 2019, pp. 5180–5186.
- [6] Y. Suga, M. Miyakami, I. Mizoguchi, and H. Kajimoto, "3d shape presentation by combination of force feedback and electro-tactile stimulation," in *2023 IEEE World Haptics Conference (WHC)*. IEEE, 2023, pp. 361–367.
- [7] E. J. Gonzalez, E. Ofek, M. Gonzalez-Franco, and M. Sinclair, "X-rings: A hand-mounted 360 shape display for grasping in virtual reality," in *Proceedings of the 34th Annual Symposium on User Interface Software and Technology*, 2021, pp. 732–742.
- [8] Y. Sun, S. Yoshida, T. Narumi, and M. Hirose, "Pacapa: A handheld vr device for rendering size, shape, and stiffness of virtual objects in tool-based interactions," in *Proceedings of the 2019 CHI Conference on Human Factors in Computing Systems*, 2019, pp. 1–12.
- [9] CyberGlove, "Cybergrip," <https://www.cyberglovesystems.com/cybergrip>, 1990, accessed: May 12, 2025.
- [10] C. Fang, Y. Zhang, M. Dworman, and C. Harrison, "Wireality: Enabling complex tangible geometries in virtual reality with worn multi-string haptics," in *Proceedings of the 2020 CHI Conference on Human Factors in Computing Systems*, 2020, pp. 1–10.
- [11] T. Feix, J. Romero, H.-B. Schmiedmayer, A. M. Dollar, and D. Kragic, "The grasp taxonomy of human grasp types," *IEEE Transactions on Human-Machine Systems*, vol. 46, no. 1, pp. 66–77, 2015.
- [12] T. Feix, I. M. Bullock, and A. M. Dollar, "Analysis of human grasping behavior: Object characteristics and grasp type," *IEEE Transactions on Haptics*, vol. 7, no. 3, pp. 311–323, 2014.
- [13] K.-S. Lee and M.-C. Jung, "Common patterns of voluntary grasp types according to object shape, size, and direction," *International Journal of Industrial Ergonomics*, vol. 44, no. 5, pp. 761–768, 2014.
- [14] J. Martínez, A. García, M. Oliver, J. P. Molina, and P. González, "Identifying virtual 3d geometric shapes with a vibrotactile glove," *IEEE Computer Graphics and Applications*, vol. 36, no. 1, pp. 42–51, 2014.
- [15] A. Frisoli, M. Solazzi, M. Reiner, and M. Bergamasco, "The contribution of cutaneous and kinesthetic sensory modalities in haptic perception of orientation," *Brain Research Bulletin*, vol. 85, no. 5, pp. 260–266, 2011.
- [16] I. Sarakoglou, A. Brygo, D. Mazzanti, N. G. Hernandez, D. G. Caldwell, and N. G. Tsagarakis, "Hexotrac: A highly under-actuated hand exoskeleton for finger tracking and force feedback," in *2016 IEEE/RSJ International Conference on Intelligent Robots and Systems (IROS)*. IEEE, 2016, pp. 1033–1040.
- [17] P. Agarwal, J. Fox, Y. Yun, M. K. O'Malley, and A. D. Deshpande, "An index finger exoskeleton with series elastic actuation for rehabilitation: Design, control and performance characterization," *The International Journal of Robotics Research*, vol. 34, no. 14, pp. 1747–1772, 2015.
- [18] Y. Zhang, D. Wang, Z. Wang, Y. Zhang, and J. Xiao, "Passive force-feedback gloves with joint-based variable impedance using layer jamming," *IEEE Transactions on Haptics*, vol. 12, no. 3, pp. 269–280, 2019.
- [19] H. Yang, D. K. Patel, T. Johnson, K. Zhong, G. Olson, C. Majidi, M. F. Islam, T. Zhang, and L. Yao, "A compliant metastructure design with reconfigurability up to six degrees of freedom," *Nature Communications*, vol. 16, no. 1, p. 719, 2025.
- [20] L. A. Jones and A. M. Smith, "Tactile sensory system: encoding from the periphery to the cortex," *Wiley Interdisciplinary Reviews: Systems Biology and Medicine*, vol. 6, no. 3, pp. 279–287, 2014.
- [21] S. Baik, S. Park, and J. Park, "Corrigendum: Haptic glove using tendon-driven soft robotic mechanism," *Frontiers in Bioengineering and Biotechnology*, vol. 8, p. 541105, 2020.
- [22] N. Vanichvoranun, H. Lee, S. Kim, and S. H. Yoon, "Estatig: Wearable haptic feedback with multi-phalanx electrostatic brake for enhanced object perception in vr," *Proceedings of the ACM on Interactive, Mobile, Wearable and Ubiquitous Technologies*, vol. 8, no. 3, pp. 1–29, 2024.
- [23] F. A. Geldard and C. E. Sherrick, "The cutaneous 'rabbit': a perceptual illusion," *Science*, vol. 178, no. 4057, pp. 178–179, 1972.
- [24] D. S. Alles, "Information transmission by phantom sensations," *IEEE Transactions on Man-Machine Systems*, vol. 11, no. 1, pp. 85–91, 1970.
- [25] H. Luo, Z. Wang, Z. Wang, Y. Zhang, and D. Wang, "Perceptual localization performance of the whole hand vibrotactile funneling illusion," *IEEE Transactions on Haptics*, vol. 16, no. 2, pp. 240–250, 2023.
- [26] M. Miyazaki, M. Hirashima, and D. Nozaki, "The 'cutaneous rabbit' hopping out of the body," *Journal of Neuroscience*, vol. 30, no. 5, pp. 1856–1860, 2010.
- [27] G. Park, H. Cha, and S. Choi, "Haptic enchanters: Attachable and detachable vibrotactile modules and their advantages," *IEEE Transactions on Haptics*, vol. 12, no. 1, pp. 43–55, 2018.
- [28] H. Lee, E. Kim, and S. H. Yoon, "3d shape perception through spatiotemporal vibrotactile patterns with kinesthetic feedback," in *2025 IEEE World Haptics Conference (WHC)*. IEEE, 2025, pp. 439–445.
- [29] J. P. Warren, M. Santello, and S. I. Helms Tillery, "Effects of fusion between tactile and proprioceptive inputs on tactile perception," *PLoS One*, vol. 6, no. 3, p. e18073, 2011.
- [30] K. O. Johnson, "The roles and functions of cutaneous mechanoreceptors," *Current Opinion in Neurobiology*, vol. 11, no. 4, pp. 455–461, 2001.
- [31] Z. Zhakypov and A. M. Okamura, "Fingerprint: A 3-d printed soft monolithic 4-degree-of-freedom fingertip haptic device with embedded actuation," in *2022 IEEE 5th International Conference on Soft Robotics (RoboSoft)*. IEEE, 2022, pp. 938–944.
- [32] B. Lim, K. Kim, and D. Hwang, "On the design of the 5-dof finger-wearable cutaneous haptic device," in *2017 IEEE International Conference on Robotics and Biomimetics (ROBIO)*. IEEE, 2017, pp. 872–878.
- [33] D. Prattichizzo, F. Chinello, C. Pacchierotti, and M. Malvezzi, "Towards wearability in fingertip haptics: a 3-dof wearable device for cutaneous force feedback," *IEEE Transactions on Haptics*, vol. 6, no. 4, pp. 506–516, 2013.
- [34] C. Park, Y. Lee, and S. H. Yoon, "Ultraboard: Always-available wearable ultrasonic mid-air haptic interface for responsive and robust vr inputs," *Proceedings of the ACM on Interactive, Mobile, Wearable and Ubiquitous Technologies*, vol. 9, no. 2, pp. 1–31, 2025.
- [35] R. Kovacs, E. Ofek, M. Gonzalez Franco, A. F. Siu, S. Marwecki, C. Holz, and M. Sinclair, "Haptic pivot: On-demand handhelds in vr," in *Proceedings of the 33rd annual ACM symposium on user interface software and technology*, 2020, pp. 1046–1059.
- [36] X. de Tinguy, T. Howard, C. Pacchierotti, M. Marchal, and A. Lécuyer, "Weatavix: wearable actuated tangibles for virtual reality experiences," in *International Conference on Human Haptic Sensing and Touch Enabled Computer Applications*. Springer, 2020, pp. 262–270.
- [37] Y. Tanaka, A. Shen, A. Kong, and P. Lopes, "Full-hand electro-tactile feedback without obstructing palmar side of hand," in *Proceedings of*

- the 2023 CHI Conference on Human Factors in Computing Systems, 2023, pp. 1–15.
- [38] B. C. Stillman, “Making sense of proprioception: the meaning of proprioception, kinaesthesia and related terms,” *Physiotherapy*, vol. 88, no. 11, pp. 667–676, 2002.
- [39] P. Polygerinos, Z. Wang, K. C. Galloway, R. J. Wood, and C. J. Walsh, “Soft robotic glove for combined assistance and at-home rehabilitation,” *Robotics and Autonomous Systems*, vol. 73, pp. 135–143, 2015.
- [40] J. Qi, F. Gao, G. Sun, J. C. Yeo, and C. T. Lim, “Haptiglove—untethered pneumatic glove for multimode haptic feedback in reality–virtuality continuum,” *Advanced Science*, vol. 10, no. 25, p. 2301044, 2023.
- [41] HaptX, “Haptx gloves,” <https://haptx.com/>, accessed: May 12, 2025.
- [42] SenseGlove, “Nova 2,” <https://www.senseglove.com/product/nova-2/>, accessed: May 12, 2025.
- [43] M. Jo, D. Kwak, and S. H. Yoon, “Wrimoucon: Wrist-mounted haptic controller for rendering physical properties in virtual reality,” in *2023 IEEE World Haptics Conference (WHC)*. IEEE, 2023, pp. 34–40.
- [44] R. Hinchet, V. Vechev, H. Shea, and O. Hilliges, “Dextres: Wearable haptic feedback for grasping in vr via a thin form-factor electrostatic brake,” in *Proceedings of the 31st Annual Symposium on User Interface Software and Technology*, 2018, pp. 901–912.
- [45] bHaptics, “Tactglove,” <https://www.bhaptics.com/tactsuit/tactglove-dk2/>, accessed: May 12, 2025.
- [46] P. Preechayasomboon and E. Rombokas, “Haplets: Finger-worn wireless and low-encumbrance vibrotactile haptic feedback for virtual and augmented reality,” *Frontiers in Virtual Reality*, vol. 2, p. 738613, 2021.
- [47] G. Park and S. Choi, “Tactile information transmission by 2d stationary phantom sensations,” in *Proceedings of the 2018 CHI Conference on Human Factors in Computing Systems*, 2018, pp. 1–12.
- [48] D. S. Alles, “Information transmission by phantom sensations,” *IEEE Transactions on Man-Machine Systems*, vol. 11, no. 1, pp. 85–91, 1970.
- [49] J. Cha, L. Rahal, and A. El Saddik, “A pilot study on simulating continuous sensation with two vibrating motors,” in *2008 IEEE International Workshop on Haptic Audio visual Environments and Games*.
- [50] C. E. Sherrick and R. Rogers, “Apparent haptic movement,” *Perception & Psychophysics*, vol. 1, no. 3, pp. 175–180, 1966.
- [51] B. Remache-Vinueza, A. Trujillo-León, and F. Vidal-Verdú, “Phantom sensation: Threshold and quality indicators of a tactile illusion of motion,” *Displays*, vol. 83, p. 102676, 2024.
- [52] T. Bagneschi, D. Chiaradia, G. Righi, G. Del Popolo, A. Frisoli, and D. Leonardis, “A soft hand exoskeleton with a novel tendon layout to improve stable wearing in grasping assistance,” *IEEE Transactions on Haptics*, vol. 16, no. 2, pp. 311–321, 2023.
- [53] B. B. Kang, H. Lee, H. In, U. Jeong, J. Chung, and K.-J. Cho, “Development of a polymer-based tendon-driven wearable robotic hand,” in *2016 IEEE International Conference on Robotics and Automation (ICRA)*. IEEE, 2016, pp. 3750–3755.
- [54] P. K. D. Tran, P. V. A. Gadepalli, J. Lee, and A. S. Nittala, “Augmenting on-body touch input with tactile feedback through fingernail haptics,” in *Proceedings of the 2023 CHI Conference on Human Factors in Computing Systems*, 2023, pp. 1–13.
- [55] G. Serhat and K. J. Kuchenbecker, “Fingertip dynamic response simulated across excitation points and frequencies,” *Biomechanics and Modeling in Mechanobiology*, vol. 23, no. 4, pp. 1369–1376, 2024.
- [56] G. Serhat and K. J. Kuchenbecker, “Free and forced vibration modes of the human fingertip,” *Applied Sciences*, vol. 11, no. 12, p. 5709, 2021.
- [57] T. Hulin, M. Rothhammer, I. Tannert, S. Subramanyam Giri, B. Pleintinger, H. Singh, B. Weber, and C. Ott, “Fingertac—a wearable tactile thimble for mobile haptic augmented reality applications,” in *International Conference on Human-Computer Interaction*. Springer, 2020, pp. 286–298.
- [58] B. B. Kang, H. Choi, H. Lee, and K.-J. Cho, “Exo-glove poly ii: A polymer-based soft wearable robot for the hand with a tendon-driven actuation system,” *Soft Robotics*, vol. 6, no. 2, pp. 214–227, 2019.
- [59] H. In, B. B. Kang, M. Sin, and K.-J. Cho, “Exo-glove: A wearable robot for the hand with a soft tendon routing system,” *IEEE Robotics & Automation Magazine*, vol. 22, no. 1, pp. 97–105, 2015.
- [60] R. S. Johansson and A. B. Vallbo, “Tactile sensibility in the human hand: relative and absolute densities of four types of mechanoreceptive units in glabrous skin,” *The Journal of Physiology*, vol. 286, no. 1, pp. 283–300, 1979.
- [61] M. R. Cutkosky *et al.*, “On grasp choice, grasp models, and the design of hands for manufacturing tasks,” *IEEE Transactions on Robotics and Automation*, vol. 5, no. 3, pp. 269–279, 1989.
- [62] S. Sathiyamurthy, M. Lui, E. Kim, and O. Schneider, “Measuring haptic experience: Elaborating the hx model with scale development,” in *2021 IEEE World Haptics Conference (WHC)*. IEEE, 2021, pp. 979–984.
- [63] W. M. B. Tiest and A. M. Kappers, “Cues for haptic perception of compliance,” *IEEE Transactions on Haptics*, vol. 2, no. 4, pp. 189–199, 2009.
- [64] J. K. Gibbs, M. Gillies, and X. Pan, “A comparison of the effects of haptic and visual feedback on presence in virtual reality,” *International Journal of Human-Computer Studies*, vol. 157, p. 102717, 2022.
- [65] M. O. Ernst and M. S. Banks, “Humans integrate visual and haptic information in a statistically optimal fashion,” *Nature*, vol. 415, no. 6870, pp. 429–433, 2002.
- [66] L. Rincon-Gonzalez, J. P. Warren, D. M. Meller, and S. H. Tillery, “Haptic interaction of touch and proprioception: implications for neuro-prosthetics,” *IEEE Transactions on Neural Systems and Rehabilitation Engineering*, vol. 19, no. 5, pp. 490–500, 2011.
- [67] Google, “Mediapipe,” <https://developers.google.com/mediapipe>, 2023, accessed: March 6, 2026.
- [68] M. Ferre, I. Galiana, R. Wirz, and N. Tuttle, “Haptic device for capturing and simulating hand manipulation rehabilitation,” *IEEE/ASME Transactions on Mechatronics*, vol. 16, no. 5, pp. 808–815, 2011.



Hojeong Lee is a Ph.D. Candidate in the Robotics Program, KAIST. She received the Master’s degree from the Graduate School of Culture Technology, KAIST, and the B.S. from the College of Fine Arts, Seoul National University. Her research focuses on developing wearable haptic devices with a control system for haptic rendering, considering natural interaction scenarios.



Eunho Kim received the B.S. degree in Mechanical Engineering from Yonsei University and is currently a Master’s student at the HCI Tech Lab, Graduate School of Culture Technology, KAIST. His research focuses on Human-Robot Interaction and haptics, developing natural user interactions for enhanced perception and social connection.



Rachel Kim is a Master’s student at the HCITech Lab in the School of Computing at KAIST, where she also received her B.S. degree. Her research interests focus on interaction design and the development of natural user interactions, particularly for mobile and XR interfaces.



Sang Ho Yoon is an Associate Professor with the Graduate School of Culture Technology, KAIST, where he leads the HCI Tech Lab. Prior to joining KAIST, he was a Principal Engineer at Samsung Research and a Research Engineer at Microsoft Applied Sciences Lab. He received the Ph.D. degree from Purdue University, and the B.S. and M.S. degrees from Carnegie Mellon University. His research focuses on developing natural user interactions that address physical, mental, and social barriers with novel haptic interfaces and sensing techniques.